



## Review Article



# Do multiheme cytochromes containing close-packed heme groups have a band structure formed from the heme $\pi$ and $\pi^*$ orbitals?

Jessica H. van Wonderen<sup>1</sup>, Alejandro Morales-Florez<sup>1</sup>, Thomas A. Clarke<sup>1</sup>, Andrew J. Gates<sup>1</sup>, Jochen Blumberger<sup>2</sup>, Zdenek Futera<sup>3</sup>, David J. Richardson<sup>1</sup>, Julea N. Butt<sup>1,4</sup> and Geoffrey R. Moore<sup>4</sup>

## Abstract

Multiheme cytochromes (MHCs) are bacterial electron-transfer proteins. We show from optical spectra and calculations that some of these cytochromes probably contain occupied and unoccupied bands formed from heme  $\pi$  and  $\pi^*$  orbitals that span the protein. In the fully oxidised proteins, the unoccupied  $\pi^*$ -bands are energetically above the redox-active frontier orbitals, which according to NMR data and calculations, are formed of  $\text{Fe}^{3+} t_{2g}$  and porphyrin  $\pi$ -orbitals. These orbitals on different hemes are electronically coupled according to EPR data and calculations, but only weakly so. We suggest a role for the heme bands in the electronic conductivity of single MHCs in bioelectronic junctions that is distinct from the role of the redox-active  $\text{Fe}^{3+} t_{2g}$  and porphyrin  $\pi$ -orbitals in physiological electron transfer.

## Addresses

<sup>1</sup> School of Biological Sciences, University of East Anglia, Norwich Research Park Norwich, NR4 7TJ, UK

<sup>2</sup> Department of Physics and Astronomy, University College London, London, WC1E 6BT, UK

<sup>3</sup> Faculty of Science, University of South Bohemia, Branisovska 1760, 370 05 Ceske Budejovice, Czech Republic

<sup>4</sup> School of Chemistry, University of East Anglia, Norwich Research Park Norwich, NR4 7TJ, UK

Corresponding author: Moore, Geoffrey R. ([g.moore@uea.ac.uk](mailto:g.moore@uea.ac.uk))

Current Opinion in Electrochemistry 2024, 47:101556

This review comes from a themed issue on **Bioelectrochemistry (2024)**

Edited by **Julea Butt**

For a complete overview see the [Issue](#) and the [Editorial](#)

Available online 12 June 2024

<https://doi.org/10.1016/j.coelec.2024.101556>

2451-9103/© 2024 The Authors. Published by Elsevier B.V. This is an open access article under the CC BY-NC license (<http://creativecommons.org/licenses/by-nc/4.0/>).

Given the role as Guest Editor, Julea Butt had no involvement in the peer review of the article and has no access to information regarding its peer-review. Full responsibility for the editorial process of this article was delegated to Richard Compton.

## Keywords

Cytochromes, Heme, Molecular orbitals, Band structure, Spectroscopy, Electron transfer, Electronic conductivity, Bioelectronics.

## Abbreviations

cyts, cytochromes *c*; HEPES, 4-(2-hydroxyethyl)-1-piperazineethanesulfonic acid; LDAO, *N,N*-Dimethyldodecan-1-amine *N*-oxide; MHC, multiheme cytochromes *c*.

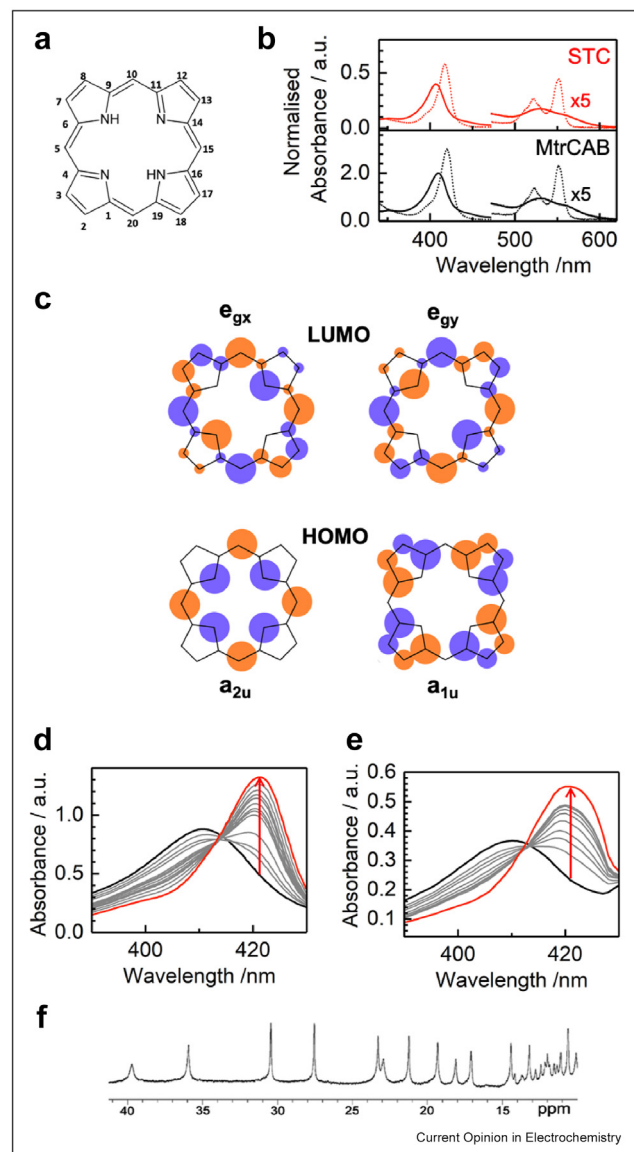
## Introduction

Extracellular respiration is a process employed by some bacteria to thrive under anaerobic conditions [1–4]. A general feature of this process is that electrons inside the cell are transported to substrates outside the cell, such as solid metal oxides. Proteins containing heme, a derivative of the porphyrin ring (Figure 1a) with  $\text{Fe}^{2+}/\text{Fe}^{3+}$  bound to the four pyrrole nitrogens are central to this. Such proteins, termed cytochromes, act as electron transfer agents both inside and outside the cell as well as across the outer membrane [1–5]. In this article we review spectroscopic data (Figure 1) for cytochromes involved in extracellular respiration that contain more than one heme to address the issue of how orbitals of the heme groups interact with each other and with the redox-active orbitals of the  $\text{Fe}^{3+}$  ions, report initial molecular orbital calculations for how the heme groups may interact, and consider the implications our findings have for the functions of the proteins. In doing this we draw on a considerable body of work involving small molecules and monoheme proteins, both theoretical and experimental, some going back more than 60 years.

## Classification and structures of multiheme cytochromes

Cytochromes *c* (cyts) contain at least one heme formed from a protoporphyrin IX (Figure 1a). Usually a Cys-X-X-Cys-His motif is the heme-binding site: the Cys residues make thioether linkages with the vinyl substituents of the protoporphyrin, and the His coordinates to the iron [6]. In some cyts the iron is 5-coordinate and in others it is 6-coordinate, generally with an additional His or Met as an axial ligand. While many cyts contain only one heme-

Figure 1



(a) The Fischer structure of porphyrin. Protoporphyrin IX has four  $-\text{CH}_3$  substituents (at positions 3, 8, 13 and 17), two  $-\text{CH}=\text{CH}_2$  substituents (at positions 7 and 12), and two  $-\text{CH}_2-\text{CH}_2-\text{CO}_2\text{H}$  substituents (at positions 2 and 18). In c-type cytochromes the vinyl groups react with the thiol side chains of Cys residues to form thioether links to the protein. (b) UV-visible absorbance spectra of fully oxidised (solid lines) and fully reduced (dotted lines) STC (red, upper panel) and MtrCAB (black, lower panel) using a bandwidth and data interval of 0.1 nm, 200 nm/min and 0.06 s response time (JASCO V-770 spectrophotometer). The peak widths at half peak height for the Soret bands of the tetraheme STC and icoheme MtrCAB are the same. (c) The four-orbital model by Gouterman shows the porphyrin HOMOs and LUMOs. The orange and blue spheres represent different phases of the orbitals with the size of the spheres indicating the relative electron densities (picture licensed under Creative Commons, cc by-nc-sa 3.0) [7]. The HOMOs,  $a_{1u}$  and  $a_{2u}$  orbitals, are non-degenerate, but close in energy, and the LUMOs are a degenerate pair of  $e_g$  orbitals. (d) UV-visible absorbance spectra for the gradual reduction of MtrC from oxidised (black solid line) to fully reduced (red solid line), slit width and sampling interval both 1 nm. All experiments

binding motif, multiheme cytochromes c (MHCs) are common in bacteria [8–11]. Nomenclature for monoheme cyts is well established [6], but there is not an accepted classification scheme for MHCs. The InterPro database [12] has 31 entries in its MHC superfamily (IPRO36280). In this review we are concerned with members of the IPRO12286 and IPRO20014 families (Table 1), for which the hemes are 6-coordinate.

In the small tetraheme cytochrome STC from *Shewanella oneidensis* [13–15] the central pair of hemes are approximately parallel to each other and in van der Waals contact but are displaced relative to each other, so they are not completely co-planar (Figure 2a). Each of the other hemes is roughly orthogonal to one of the parallel hemes, creating a T-shaped motif. These two packing motifs, the displaced parallel and T-shaped, first described for cytochrome  $c_{554}$  from *Nitrosomonas europaea* [16], are present in other proteins listed in Table 1. For example, the 10 hemes of MtrC (Figure 2b and c) form a central core of four almost co-planar hemes (hemes 1, 2, 6 and 7) with the remaining six hemes forming T-shaped motifs with themselves and for two of them (hemes 3 and 8), with the four almost parallel hemes [17].

Aromatic amino acids in proteins adopt preferential packing interactions with other aromatic residues [18–20] in agreement with theoretical studies that suggests the preferred orientation of a benzene dimer is the parallel staggered orientation with the T-shaped orientation having a higher energy [21]. The reason these motifs are common is the presence of  $\pi$ -orbitals, which enhances the attraction one aromatic group has for another at relatively long distances [22], a factor which should also influence the packing of heme groups, which is why the displaced parallel and T-shaped motifs are prevalent.

performed with 0.7  $\mu\text{M}$  protein in 100 mM HEPES buffer pH8 with 5 mM LDAO, 150 mM NaCl. Chemical reductions were performed anaerobically using sodium dithionite (2 mg/mL). Note the isosbestic points, consistent with the oxidised hemes within a protein having the same wavelength maxima and similarly the reduced hemes within a protein. (e) Ru-MtrC:MtrAB (0.14  $\mu\text{M}$ ) in anaerobic 50 mM Tris, 10 mM KCl, 100 mM EDTA, 0.2% (v/v) Triton X-100, pH 8.5. Irradiation at 450 nm, intensity 110  $\text{Wm}^{-2}$ . Replotted from Ref. [23] with oxidised MtrCAB (solid black line), photo-reduced MtrCAB over time (grey lines) and fully reduced MtrCAB (solid red line). Spectra were recorded using a Biochrom WPA Biowave II Diode-array UV/Vis spectrophotometer under  $\text{N}_2$  with an Omega Optical 475RB Notch filter to prevent photoexcitation of RuMe by the spectrophotometer. The band width was 10 nm. (f) High frequency region of the  $1\text{D-}^1\text{H}$  NMR spectra of oxidised STC at pH 7.0 and 25  $^\circ\text{C}$  [24]  $^1\text{H}$  NMR signals of diamagnetic proteins generally fall in the chemical shift range of 0–10 ppm. The STC peaks from 15 to 40 ppm come from groups affected by the paramagnetism of the  $\text{Fe}^{3+}$ -hemes. Many of the signals are from heme methyl groups that experience a contact shift resulting from spin density of the  $\text{Fe}^{3+}$  entering porphyrin orbitals. Reproduced with permission.

Table 1

Multiheme cytochromes *c.*

Cytochrome	Number of hemes	Subcellular location	Oxidised Soret maximum/nm	Reduced Soret maximum/nm	Reduced $\alpha$ maximum/nm	References
STC	4	Periplasmic	407.2	417.5	551.7	[14]
MtrA	10	Periplasmic <sup>a</sup>	407.5	419.3	552.9	[25,26]
MtrC	10	Extracellular	410.0	420.1	551.6	[17]
OmcA	10	Extracellular	409.4	419.6	550.9	[27]
UndA	11	Extracellular	410.5	420.1	551.2	[28]
MtrAB	10	Integral OM complex	408.1	418.9	552.6	[25,26]
MtrCAB	20	Integral OM complex with extracellular domain	410.1	420.0	551.3	[25]

Oxidised and reduced Soret maximum and  $\alpha$  maximum from UV–visible absorbance of cyts using a bandwidth and data interval of 0.1 nm, 200 nm/min and 0.06 s response time (JASCO V-770 spectrophotometer). All experiments performed with 0.7  $\mu$ M protein in 100 mM HEPES, pH7, 100 mM NaCl, and with 5 mM LDAO at 20 °C. Chemical reductions were performed anaerobically with aliquots of anaerobic sodium dithionite (2 mg/mL).

<sup>a</sup> Engineered periplasmic form expressed in *Shewanella oneidensis* (PhD thesis, Matthew Lawes, University of East Anglia, 2015).

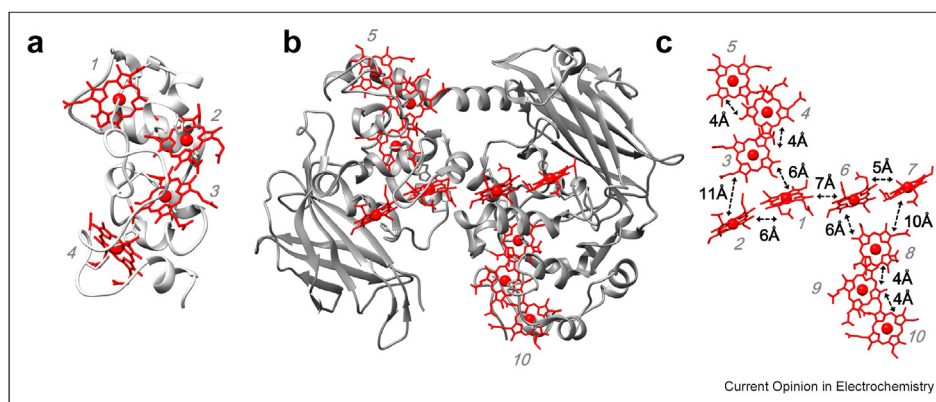
## Spectroscopy of multiheme cytochromes

## UV-visible spectroscopy

UV-visible spectroscopy has been invaluable in characterising cytochromes, as the spectra of reduced and oxidised STC [13,15] and MtrCAB [25] illustrate (Figure 1b). The absorption bands arise from electronic transitions involving the protoporphyrin  $\pi$  and  $\pi^*$  orbitals. Gouterman [29–31] developed a molecular orbital scheme to account for these involving two HOMOs and two LUMOs (Figure 1c). He showed that the two transitions,  $a_{1u} \rightarrow e_g$  and  $a_{2u} \rightarrow e_g$ , mixed to give an intense band, the Soret band at ca. 407–420 nm, and a weaker set of bands, the  $\alpha$  and  $\beta$  bands at ca. 500–560 nm (Table 1). The  $\alpha$  and  $\beta$  bands arise from the same electronic transition but different C–C stretching mode vibrational transitions:  $\alpha$  is a (0,0) and  $\beta$  a (0,1) transition. This scheme is still the accepted theoretical explanation for the UV–visible spectra of hemes [32–34].

A striking feature for all the proteins listed in Table 1 is that the heme groups within each protein have the same spectra in terms of the wavelengths of their Soret,  $\alpha$  and  $\beta$  bands. This is shown by UV–visible spectra of the proteins as they are gradually reduced from their fully oxidised states (Figure 1d and e show examples). Note that this identity in spectra is independent of the method of reduction since, for example, spectral identity exists for proteins reduced electrochemically [35], by photoreduction in the presence of photosensitisers [36], and with dithionite in the presence of redox mediators [37]. The spectral identity of the heme groups in these proteins is not because they are all bis-His coordinated because the proteins we are considering have different spectra from each other (Table 1). For example, the Soret band for the 10 hemes of MtrA shifts to longer wavelengths in MtrCAB and have the same wavelength maximum as the 10 hemes of the bound MtrC (Table 1).

Figure 2



X-ray crystal structures of (a) STC (pdb: 1M1Q) and (b) MtrC (pdb: 4LM8) with the hemes depicted in red. (c) Staggered-cross heme structure of MtrC with the hemes numbered (grey italics) and the heme-to-edge distances shown.

We suggest that the spectral identity of the heme groups within a single protein is a consequence of the formation of bands of molecular orbitals involving all the heme groups within the protein so that the energies of the Soret  $\pi \rightarrow \pi^*$  transitions are the same, as are the energies of the  $\alpha/\beta \pi \rightarrow \pi^*$  transitions. Figure 2 shows that the heme groups of STC and MtrC are close enough for their four Gouterman molecular orbitals to interact. A full MO treatment of such interactions is beyond the scope of this paper, though we find from calculated molecular orbitals for a monomer and a dimer of bis-His coordinated  $\text{Fe}^{3+}$ -porphin that the  $a_{1u}$  orbitals on each monomer combine symmetrically and antisymmetrically, and similarly for  $a_{2u}$  and  $e_g$  orbitals (Figure 3). In longer heme chains these combinations would give rise to the formation of narrow occupied and unoccupied bands.

The electronic coupling between the hemes to create the occupied and unoccupied bands is relatively weak. We know this because the electronic transition energies in the UV–visible spectra are like those of monoheme

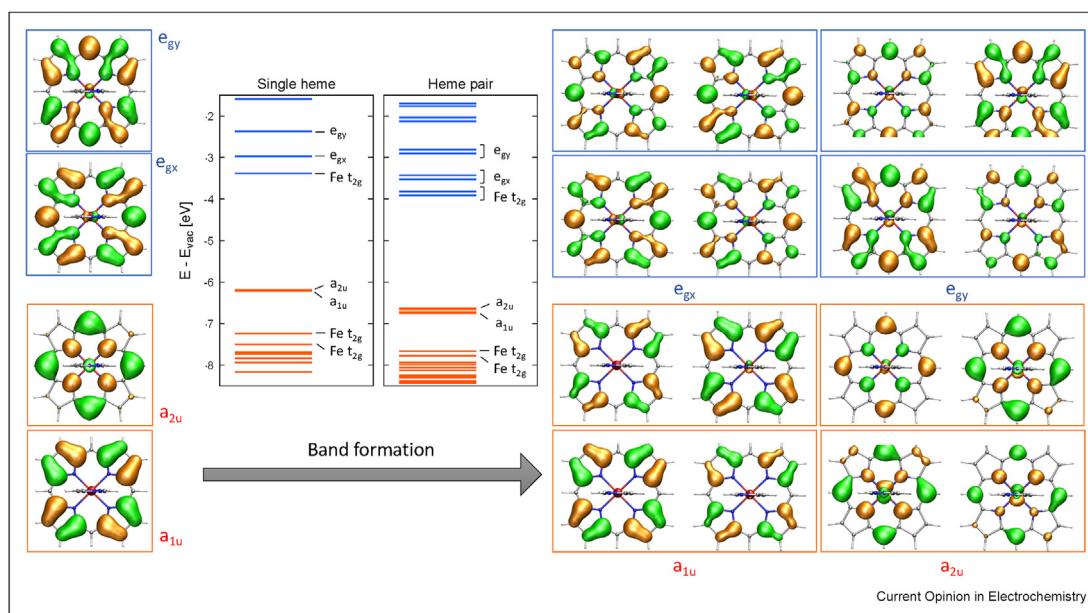
cytochromes. Furthermore, Posligua et al. [38] calculated that fused porphyrin polymers without a linking group had a metallic band structure, while porphyrins linked by ethyne or butadiyne had small band gaps that increased with the number of carbons, demonstrating that the coupling between hemes is the key determinant of band gap.

It will be interesting to discover when a transition from individual heme HOMOs and LUMOs, to a manifold of heme HOMOs and LUMOs, and then, perhaps, onto a valence band and conduction band occurs. It is not just the number of hemes that will be relevant for this as the tetraheme STC seems to have a band structure, as we have shown, while published optical spectra of tetraheme cytochromes  $c_3$  [6,39], which have a different packing of hemes [39], show no evidence of a band structure.

### NMR spectroscopy

$^1\text{H}$  NMR spectra of ferricytochromes, including STC [24,40] (Figure 1f), OmcA [41] and triheme and

Figure 3



Calculated molecular orbital energy level diagram for a monomer and a dimer of bis-His coordinated  $\text{Fe}^{3+}$  porphin. Occupied (unoccupied) energy levels are shown in orange (blue). The energy levels of the occupied Gouterman orbitals  $a_{1u}$ ,  $a_{2u}$ , unoccupied Gouterman orbitals  $e_{gx}$ ,  $e_{gy}$  and the  $\text{Fe}^{3+} t_{2g}$  orbitals are indicated. In the dimer, the Gouterman orbitals form symmetric and antisymmetric combinations (orbitals depicted to the right of the figure) which in the case of a linear heme chain would result in band formation. The  $e_{gy}$  orbital is not equally delocalized over both monomers due to numerical inaccuracies of the calculations. Notice that in the oxidized state the occupied Gouterman orbitals are predicted to be higher in energy than the occupied  $\text{Fe}^{3+} t_{2g}$  orbitals, thus forming the HOMO, whilst the unoccupied  $\text{Fe}^{3+} t_{2g}$  orbital is predicted to be lower in energy than the unoccupied Gouterman orbitals, thus forming the LUMO. Notice also that the degeneracy of the unoccupied Gouterman  $e_g$  orbitals appears to be lifted, possibly due to symmetry breaking. In the dimer, the porphin planes are parallel and the Fe–Fe distance is 11 Å corresponding to a heme-edge to heme-edge distance of 4.02 Å. The heme orientation is such that one heme is the mirror image of the other with the  $\delta\text{N}$  of the axial histidines facing one another. The calculations were carried out with the PBE0 density functional in the doublet spin state for the bis-His  $\text{Fe}^{3+}$ -porphin monomer and in the triplet spin state for the bis-His  $\text{Fe}^{3+}$ -porphin dimer using a TZVP-MOLOPT-SR basis set for  $\text{Fe}^{3+}$  and TZV2P-MOLOPT basis set for H, N, C, ADMM basis cFIT13 for Fe and cFIT3 for H, C, N, GTH pseudopotentials (16 electron valence for Fe, 1 for H, 4 for C and 5 for N) and a 350  $R_y$  cutoff for the reciprocal grid. Only the energy levels for the minority spin electrons in the given energy range are shown. The calculations were carried out with the CP2K programme package [42].

hexaheme domains of the periplasmic dodecaheme cyt GSU1996 from *Geobacter sulfurreducens* [43], show that unpaired electron spin density from the  $\text{Fe}^{3+}$  creates large chemical shift perturbations via scalar (contact) and dipolar (pseudocontact) interactions [44–47]. Contact shifts result from spin density being delocalised into the porphyrin and the axial ligands. Note that the spin delocalisation we are considering is the transfer of small fractions of an unpaired electron from the metal to the porphyrin and not the complete transfer of an electron.

$\text{Fe}^{3+}$  d-orbitals can mix with porphyrin  $\pi$  and  $\pi^*$  orbitals, and how they do this depends on the electron occupancy of the d-orbitals and on the energies and symmetries of the relevant orbitals, which in turn depends on issues such as whether the heme is distorted and the identity of the axial ligands [46–50]. In a tetragonal crystal field, the  $t_{2g}$  set of three d-orbitals split further, and for low-spin monoheme cytochromes that have been characterised the unpaired electron is in the  $d_{xz}/d_{yz}$  pair of orbitals, which lie perpendicular to the plane of the heme and interact with the porphyrin  $\pi$ -orbitals [48,50,51]. For heme compounds containing low-spin  $\text{Fe}^{3+}$  X-ray absorption spectroscopy suggests the electron delocalisation into the porphyrin occurs by what Solomon and his colleagues call a ‘hole superexchange pathway’ [52].

### EPR spectroscopy

EPR studies reported additional surprising results in that spin–spin coupling between  $\text{Fe}^{3+}$  ions in some of the heme groups of MtrC is observed [37]. In principle, such spin–spin coupling could be scalar or dipolar in origin. However, EPR studies of other close-packed MHCs, such as the tetraheme cytochrome  $c_3$  and the tri-heme cytochrome  $c_7$ , do not exhibit spin–spin coupling between the heme  $\text{Fe}^{3+}$  ions [53,54], so we think that it is most likely such coupling is scalar. Scalar coupling requires the coupled heme groups to share electron density, and this requires electron delocalisation between hemes that could arise when  $\text{Fe}^{3+}$  d-orbitals mix with heme  $\pi$ -orbitals to form narrow bands.

In this respect, it is important to note that while we propose that hemes have lost their individual identities as far as their  $\pi$  and  $\pi^*$  orbitals are concerned, they have not lost their identities as far as the  $\text{Fe}^{2+}/\text{Fe}^{3+}$  ions and the substituents to the hemes are concerned. This is shown by the multitude of signals in EPR spectra of ferric MtrC [37] and the  $^1\text{H}$  NMR spectra of STC and GSU1996 [24,40,43], and by the observation of different redox potentials for different hemes [8,13,37,24,40,55] This is an important observation because the d-orbitals of the  $\text{Fe}^{2+}/\text{Fe}^{3+}$  ions are the primary redox orbitals of the proteins.

### Mechanistic implications of a band structure in multiheme cytochromes

Long-range electron transfer in proteins is generally discussed in terms of hopping and tunnelling mechanisms [56–58] but without a full MO description of the band structure in our MHCs, it is not possible to be certain about mechanistic implications. However, we can make pertinent observations. Firstly, we note that though the proposed bands explain the electronic spectral identity of the hemes within a protein we have no evidence that they are involved in electron transfer. For this reason, we term the band formed from  $\pi$ -orbitals the occupied band and the band involving the  $\pi^*$ -orbitals the unoccupied band. Secondly, we note that the proteins of Table 1 have some of the fastest inter-heme electron transfer rates reported [59], and, so far, are the only proteins suggested to have a band structure formed by porphyrin orbitals, as described in Section UV-visible spectroscopy. Of course, this could be a coincidence, but this is a matter that should be explored further.

The bands formed by heme orbitals could also play a pivotal role in the electronic conduction of MHCs [38,55,60]. Recent measurements on junctions of STC and MtrF have shown that the electronic conductance of the proteins was temperature independent from room temperature down to below 100 K [38]. This observation could only be explained by a coherent tunnelling model where conductance is mediated by delocalized ‘band-like’ states [55,60]. Notice that during the tunnelling process the protein does not get oxidized or reduced. The transferring electron resides on the protein only on the electronic time scale (femtosecond or lower), not on the time scale of nuclear vibrations. Calculations on Au-STC-Au junctions showed that the ‘band-like’ states mediating tunnelling were typically delocalized over 2–3 heme cofactors, bridging the gap between the two electrodes, and over protein amino acids interacting with the electrodes [61], suggesting that these ‘band-like’ states involve our proposed heme bands.

It is important to note that the biological roles of the MHCs are to transfer electrons between proteins and from proteins to electron-accepting substrates, and many *in vitro* experiments with these proteins are aimed at determining how they carry out their physiological functions e.g. Ref. [59]. We would like to emphasize that the physics of biological electron transfer involving molecular donors and acceptors is very different from the electronic conduction scenario involving metal electrodes as donors and acceptors described above. In biological electron transfer the redox potentials of physiological electron donors and acceptors are well matched with the redox potentials of the hemes so that

electron injection into the heme chain is energetically feasible. Calculations have shown that the dielectric response of surrounding protein and water (reorganization free energy typically 0.7–1.0 eV) [62] is much larger than the electronic coupling between the redox-active Fe-d  $t_{2g}$ -porphyrin  $\pi$ -orbitals on neighbouring heme cofactors (typically only a few meV and <10 meV [62]). This causes the electron to localize on single heme cofactors and heme-to-heme hopping to be the transport mechanism. The electron transfer rates predicted by calculations [62] were subsequently found to be in good agreement with values obtained by pump probe transient absorption spectroscopy [61]. Notably, the same calculations predict that the electron hopping flux through MHCs under physiological conditions do not exceed  $10^6$ – $10^7$  s<sup>-1</sup> [62], which is more than two orders of magnitude lower than the currents measured in junctions made of the same MHC proteins [38,55], again suggesting that the conduction mechanism in protein junctions [38,55] (band-like) differs from the one in the native environment (hopping).

In the heme-to-heme hopping model, when thermal excitations bring the redox-active frontier orbitals (Fe d-heme/porphyrin  $\pi$ -orbital) of neighbouring hemes to energetic degeneracy, delocalization of these electronic states occurs temporarily over both hemes, and the electron transfers happens. In previous work we also investigated the flickering resonance mechanism [63], that is the possibility that several hemes get simultaneously into degeneracy such that delocalization of the Fe-d  $t_{2g}$ -porphyrin  $\pi$ -orbitals would be greater and longer-range hops would occur. However, we concluded that electronic coupling between the hemes is not large enough compared to their site energy fluctuations to allow such a mechanism to be feasible [64].

Finally, we draw attention to polypyrrole, which is a linear polymer with pyrrole rings linked via the C-2 carbon of one pyrrole attached to the C-5 carbon of another pyrrole [65,66]. Valence bands are formed from the  $\pi$  orbitals and conduction bands from the  $\pi^*$  orbitals. With a band gap of 3.16 eV, polypyrrole is an insulator, though p-type doped polypyrrole is a conductor [66–68]. The bands we envisage in the multiheme cytochromes come from pyrrole rings fused into a porphyrin via methine linkages between C-2 and C-5 carbons of neighbouring pyrroles, with band formation requiring both through-bond and through-space orbital overlap. It is no surprise then that the polypyrrole band gap is like the Soret and  $\alpha$  band gaps of our MHCs: 3.0 (at 410 nm) and 2.5 (at 550 nm) eV, respectively. It is beyond the scope of this article to pursue the comparison of polypyrrole and MHCs further, but we suggest it is a topic for investigation.

## Concluding remarks

We have revisited spectroscopic data on MHCs involved in extracellular respiration, some dating back almost 20 years, and have interpreted the data in the light of theoretical and experimental studies of model complexes and monoheme cytochromes, some dating back more than 60 years. Our conclusion is that the proteins we have considered contain bands of molecular orbitals that span the protein. These bands are composed of the  $\pi$  and  $\pi^*$  orbitals of the hemes and are the first such bands to be described in a protein. We went on to argue that these bands may play a role in electronic conduction of single MHCs, i.e., in bioelectronics, but are likely to be less important for physiological electron transfer functions of proteins. Future work should be directed at obtaining more evidence for the involvement of the bands in electronic conduction and in looking for possible roles for them in physiological reactions.

## Declaration of competing interest

The authors declare that they have no known competing financial interests or personal relationships that could have appeared to influence the work reported in this paper.

## Data availability

Data will be made available on request.

## Acknowledgements

We thank Professors Grant Mauk and Mike Wilson for helpful discussions, and the UK Biotechnology and Biological Sciences Research Council for financial support through the grant BB/X011453/1 and doctoral training partnership BB/T008717/1. Computational resources were supplied by the project “e-Infrastruktura CZ” (e-INFRA LM2018140) provided within the program Projects of Large Research, Development and Innovations Infrastructures. We also thank reviewers for their kind comments and helpful suggestions to improve the article.

## References

Papers of particular interest, published within the period of review, have been highlighted as:

- \* of special interest
  - \*\* of outstanding interest
1. Myers CR, Neelson KH: **Bacterial manganese reduction and growth with manganese oxide as the sole electron acceptor.** *Science* 1988, **240**:1319–1321, <https://doi.org/10.1126/science.240.4857.1319>.
  2. Gralnick JA, Newman DK: **Extracellular respiration.** *Mol Microbiol* 2007, **65**:1–11, <https://doi.org/10.1111/j.1365-2958.2007.05778.x>.
  3. Chong GW, Karbelkar AA, El-Naggar MY: **Nature's conductors: what can microbial multi-heme cytochromes teach us about electron transport and biological energy conversion?** *Curr Opin Chem Biol* 2018, **47**:7–17, <https://doi.org/10.1016/j.cbpa.2018.06.007>.
  4. Guberman-Pfeffer MJ: **To be or not to be a cytochrome: electrical characterizations are inconsistent with *Geobacter* cytochrome 'nanowires.'** *Front Microbiol* 2024, **15**, 1397124, <https://doi.org/10.3389/fmicb.2024.1397124>.

From cryo-electron microscopy structures and calculations of electron transfer rates, the author describes a model of cytochrome action that accounts for the respiratory flux of a *Geobacter sulfurreducens* cell.

5. Wang F, Gu Y, O'Brien JP, Yi SM, Yalcin SE, Srikanth V, Shen C, Vu D, Ing NL, Hochbaum AI, Egelman EH, Malvankar NS: **Structure of microbial nanowires reveals stacked hemes that transport electrons over micrometers.** *Cell* 2019, **177**:361–369.e10, <https://doi.org/10.1016/j.cell.2019.03.029>.  
Describes the 3.7 Å resolution cryo-electron microscopy structure that shows conducting nanowires of *G. sulfurreducens* are composed of polymerized hexaheme cytochrome OmcS
6. Pettigrew GW, Moore GR: *Cytochromes c: biological aspects.* Berlin: Springer-Verlag; 1987, <https://doi.org/10.1007/978-3-642-72698-9>.
7. Senge MO, Ryan AA, Letchford KA, MacGowan SA, Mielke T: **Chlorophylls, symmetry, chirality, and photosynthesis.** *Symmetry* 2014, **6**:781–843, <https://doi.org/10.3390/sym6030781>.
8. Bewley KD, Ellis KE, Firer-Sherwood MA, Elliott SJ: **Multi-heme proteins: nature's electronic multi-purpose tool.** *BBA - Bioenergetics* 2013, **1827**:938–948, <https://doi.org/10.1016/j.bbabi.2013.03.010>.
9. Edwards MJ, Richardson DJ, Paquete CM, Clarke TA: **Role of multiheme cytochromes involved in extracellular anaerobic respiration in bacteria.** *Protein Sci* 2020, **29**:830–842, <https://doi.org/10.1002/pro.3787>.
10. Salgueiro CA, Morgado L, Silva MA, Ferreira MR, Fernandes TM, Portela PC: **From iron to bacterial electroconductive filaments: exploring cytochrome diversity using *Geobacter* bacteria.** *Coord Chem Rev* 2022, **452**, 214284, <https://doi.org/10.1016/j.ccr.2021.214284>.
11. Soares R, Costa NL, Paquete CM, Andreini C, Louro RO: **A new paradigm of multiheme cytochrome evolution by grafting and pruning protein modules.** *Mol Biol Evol* 2022, **39**:1–12, <https://doi.org/10.1093/molbev/msac139>.
12. Paysan-Lafosse T, Blum M, Chuguransky S, Grego T, Pinto BL, Salazar GA, Bileschi ML, Bork P, Bridge A, Colwell L, Gough J, Haft DH, Letunic I, Marchler-Bauer A, Mi H, Natale DA, Orengo CA, Pandurangan AP, Rivoire C, Sigrist CJA, Sillitoe I, Thanki N, Thomas PD, Tosatto SCE, Wu CH, Bateman A: **InterPro in 2022.** *Nucleic Acids Res* 2023, **51**:D418–D427, <https://doi.org/10.1093/nar/gkac993>.
13. Tsapin AI, Vandenbergh I, Nealson KH, Scott JH, Meyer TE, Cusanovich MA, Harada E, Kaizu T, Akutsu H, Leys D, Van Beeumen JJ: **Identification of a small tetraheme cytochrome c and a flavocytochrome c as two of the principal soluble cytochromes c in *Shewanella oneidensis* strain MR1.** *Appl Environ Microbiol* 2001, **67**:3236–3244, <https://doi.org/10.1128/AEM.67.7.3236-3244.2001>.
14. Leys D, Meyer TE, Tsapin AS, Nealson KH, Cusanovich MA, Van Beeumen JJ: **Crystal structures at atomic resolution reveal the novel concept of “electron-harvesting” as a role for the small tetraheme cytochrome c.** *JBC* 2002, **277**:35703–35711, <https://doi.org/10.1074/jbc.M203866200>.
15. van Wonderen JH, Li D, Piper SEH, Lau CY, Jenner LP, Hall CR, Clarke TA, Watmough NJ, Butt JN: **Photosensitised multiheme cytochromes as light-driven molecular wires and resistors.** *Chembiochem* 2018, **19**:2206–2215, <https://doi.org/10.1002/cbic.201800313>.
16. Iverson T, Arciero D, Hsu B, Logan M, Hooper A, Rees D: **Heme packing motifs revealed by the crystal structure of the tetra-heme cytochrome *C<sub>554</sub>* from *Nitrosomonas europaea*.** *Nat Struct Biol* 1998, **5**:1005–1012, <https://doi.org/10.1038/2975>.  
Describes the 2.6 Å resolution X-ray structure of *Nitrosomonas europaea* cytochrome *C<sub>554</sub>* along with the first discussion of the arrangement of hemes in the MHCs we discuss.
17. Edwards MJ, White GF, Norman M, Tome-Fernandez A, Ainsworth E, Shi L, Fredrickson JK, Zachara JM, Butt JN, Richardson DJ, Clarke TA: **Redox linked flavin sites in extracellular decaheme proteins involved in microbe-mineral electron transfer.** *Sci Rep* 2015, **5**, 11677, <https://doi.org/10.1038/srep11677>.
18. Burley SK, Petsko GA: **Aromatic-aromatic interaction: a mechanism of protein structure stabilization.** *Science* 1985, **229**:23–28, <https://doi.org/10.1126/science.3892686>.
19. McGaughey GB, Gagné M, Rappé AK:  **$\pi$ -Stacking interactions. Alive and well in proteins.** *JBC* 1998, **273**:15458–15463, <https://doi.org/10.1074/jbc.273.25.15458>.
20. Lobanov MY, Pereyaslavets LB, Likhachev IV, Matkarimov BT, Galzitskaya OV: **Is there an advantageous arrangement of aromatic residues in proteins? Statistical analysis of aromatic interactions in globular proteins.** *Comput Struct Biotechnol J* 2021, **19**:5960–5968, <https://doi.org/10.1016/j.csbj.2021.10.036>.
21. Sun S, Bernstein ER: **Aromatic van der waals clusters: Structure and nonrigidity.** *J Phys Chem* 1996, **100**:13348–13366, <https://doi.org/10.1021/jp960739o>.
22. Ninković DB, Blagojević Filipović JP, Hall MB, Brothers EN, Zarić SD: **What is special about aromatic-aromatic interactions? Significant attraction at large horizontal displacement.** *ACS Cent Sci* 2020, **6**:420–425, <https://doi.org/10.1021/acscentsci.0c00005>.
23. Piper SEH, Edwards MJ, van Wonderen JH, Casadevall C, Martel A, Jeuken LJC, Reisner E, Clarke TA, Butt JN: **Bespoke biomolecular wires for transmembrane electron transfer: spontaneous assembly of a functionalized multiheme electron conduit.** *Front Microbiol* 2021, **12**, <https://doi.org/10.3389/fmicb.2021.714508>.
24. Fonseca BM, Tien M, Rivera M, Shi L, Louro RO: **Efficient and selective isotopic labeling of hemes to facilitate the study of multiheme proteins.** *Biotechniques* 2012, **52**:1–7, <https://doi.org/10.2144/000113859>.
25. Edwards MJ, White GF, Butt JN, Richardson DJ, Clarke TA: **The crystal structure of a biological insulated transmembrane molecular wire.** *Cell* 2020, **181**:665–673.e10, <https://doi.org/10.1016/j.cell.2020.03.032>.  
Describes the 2.7 Å resolution X-ray structure of the *Shewanella baltica* OS185 MtrCAB complex. The decaheme MtrA is embedded within the 26-strand  $\beta$ -barrel MtrB that crosses the outer membrane, and the decaheme MtrC is bound non-covalently to a small region of MtrA that protrudes from MtrB.
26. Edwards MJ, White GF, Lockwood CW, Lawes MC, Martel A, Harris G, Scott DJ, Richardson DJ, Butt JN, Clarke TA: **Structural modeling of an outer membrane electron conduit from a metal-reducing bacterium suggests electron transfer via periplasmic redox partners.** *JBC* 2018, **293**:8103–8112, <https://doi.org/10.1074/jbc.RA118.001850>.
27. Edwards MJ, Baiden NA, Johs A, Tomanicek SJ, Liang L, Shi L, Fredrickson JK, Zachara JM, Gates AJ, Butt JN, Richardson DJ, Clarke TA: **The X-ray crystal structure of *Shewanella oneidensis* OmcA reveals new insight at the microbe-mineral interface.** *FEBS Lett* 2014, **588**:1886–1890, <https://doi.org/10.1016/j.febslet.2014.04.013>.
28. Edwards MJ, Hall A, Shi L, Fredrickson JK, Zachara JM, Butt JN, Richardson DJ, Clarke TA: **The crystal structure of the extracellular 11-heme cytochrome UndA reveals a conserved 10-heme motif and defined binding site for soluble iron chelates.** *Structure* 2012, **20**:1275–1284, <https://doi.org/10.1016/j.str.2012.04.016>.
29. Gouterman M: **Study of the effects of substitution on the absorption spectra of porphyrin.** *J Chem Phys* 1959, **30**:1139–1161, <https://doi.org/10.1063/1.1730148>.
30. Gouterman M: **Spectra of porphyrins.** *J Mol Spectrosc* 1961, **6**:138–163, [https://doi.org/10.1016/0022-2852\(61\)90236-3](https://doi.org/10.1016/0022-2852(61)90236-3).
31. Gouterman M, Wagnière GH, Snyder LC: **Spectra of porphyrins part II. Four orbital model.** *J Mol Spectrosc* 1963, **11**:108–127, [https://doi.org/10.1016/0022-2852\(63\)90011-0](https://doi.org/10.1016/0022-2852(63)90011-0).  
Together with references 23 and 24, this describes the four-molecular orbital scheme for porphyrins that account for their UV-visible spectroscopic properties.
32. Smith DW, Williams RJP: **The spectra of ferric haems and haemoproteins.** *Struct Bond* 1970, **7**:1–45, <https://doi.org/10.1007/BFb0118898>.

33. Wamser CC, Ghosh A: **The hyperporphyrin concept: a contemporary perspective.** *JACS Au* 2022, **2**:1543–1560, <https://doi.org/10.1021/jacsau.2c00255>.
34. Simpson MC, Novikova NI: **Porphyryns: electronic structure and ultraviolet/visible absorption spectroscopy.** In *Fundamentals of porphyrin chemistry: a 21st century approach*. Edited by Brothers PJ, Senge MO, New York: Wiley; 2022:505–586, <https://doi.org/10.1002/9781119129301.ch11>.
35. Reuillard B, Ly KH, Hildebrandt P, Jeuken LJC, Butt JN, Reisner E: **High performance reduction of H<sub>2</sub>O<sub>2</sub> with an electron transport decaheme cytochrome on a porous ITO electrode.** *J Appl Collab Syst (JACS)* 2017, **139**:3324–3327, <https://doi.org/10.1021/jacs.6b12437>.
36. Ainsworth EV, Lockwood CWJ, White GF, Hwang ET, Sakai T, Gross MA, Richardson DJ, Clarke TA, Jeuken LJC, Reisner E, Butt JN: **Photoreduction of Shewanella oneidensis extracellular cytochromes by organic chromophores and dye-sensitized TiO<sub>2</sub>.** *Chembiochem* 2016, **17**:2324–2333, <https://doi.org/10.1002/cbic.201600339>.
37. Hartshorne RS, Jepson BN, Clarke TA, Field SJ, Fredrickson J, Zachara J, Shi L, Butt JN, Richardson DJ: **Characterization of Shewanella oneidensis MtrC: a cell-surface decaheme cytochrome involved in respiratory electron transport to extracellular electron acceptors.** *JBIC* 2007, **12**:1083–1094, <https://doi.org/10.1007/s00775-007-0278-y>.
- Spectroscopic, spectropotentiometric and voltammetric characterization of *Shewanella oneidensis* MtrC, with the important finding of magnetically spin-coupled low spin c-hemes.
38. Poslígua V, Aziz A, Haver R, Peeks MD, Anderson HL, Graucrespo R: **Band structures of periodic porphyrin nanostructures.** *J Phys Chem C* 2018, **122**:23790–23798, <https://doi.org/10.1021/acs.jpcc.8b08131>.
39. Moore GR, Pettigrew GW: *Cytochromes c: evolutionary, structural and physicochemical aspects*. Berlin: Springer-Verlag; 1990, <https://doi.org/10.1007/978-3-642-74536-2>.
40. Fonseca BM, Saraiva IH, Paquete CM, Soares CM, Pacheco I, Salgueiro CA, Louro RO: **The tetraheme cytochrome from Shewanella oneidensis MR-1 shows thermodynamic bias for functional specificity of the hemes.** *JBIC* 2009, **14**:375–385, <https://doi.org/10.1007/s00775-008-0455-7>.
- Assignment of the <sup>1</sup>H and <sup>13</sup>C NMR signals of the heme methyl resonances of STC from *Shewanella oneidensis* MR-1, together with identification of redox-Bohr effects associated with heme propionate ionisations, and determination of the electron distributions of partially reduced protein.
41. Neto SE, de Melo-Diogo D, Correia IJ, Paquete CM, Louro RO: **Characterization of OmcA mutants from Shewanella oneidensis MR-1 to investigate the molecular mechanisms underpinning electron transfer across the microbe-electrode interface.** *Fuel Cell* 2017, **17**:601–611, <https://doi.org/10.1002/fuce.201700023>.
42. Kühne TD, Iannuzzi M, Del Ben M, Rybkin VV, Seewald P, Stein F, Laino T, Khaliullin RZ, Schütt O, Schiffmann F, Golze D, Wilhelm J, Chulkov S, Bani-Hashemian MH, Weber V, Borstnik U, Tailliefumier M, Jakobovits AS, Lazzaro A, Pabst H, Müller T, Schade R, Guidon M, Andermatt S, Holmberg N, Schenter GK, Hehn A, Bussy A, Belleflamme F, Tabacchi G, Glöß A, Lass M, Bethune I, Mundy CJ, Plessl C, Watkins M, VandeVondele J, Krack M, Hutter J: **CP2K: an electronic structure and molecular dynamics software package - quickstep: Efficient and accurate electronic structure calculations.** *J Chem Phys* 2020, **152**, 194103, <https://doi.org/10.1063/5.0007045>.
43. Silva MA, Fernandes AP, Turner DL, Salgueiro CA: **A biochemical deconstruction-based strategy to assist the characterization of bacterial electric conductive filaments.** *Int J Mol Sci* 2023, **24**:7032, <https://doi.org/10.3390/ijms24087032>.
- Use of protein engineering to construct triheme and hexaheme domains of a dodecaheme cytochrome, and <sup>1</sup>H NMR spectroscopy to assign the heme resonances of the domains.
44. Wüthrich K: **High-resolution proton nuclear magnetic resonance spectroscopy of cytochrome c.** *PNAS USA* 1969, **63**: 1071–1078, <https://doi.org/10.1073/pnas.63.4.1071>.
- An important paper that was the first to describe the observed <sup>1</sup>H NMR chemical shifts of the methyl groups of a low-spin Fe<sup>3+</sup>-heme in terms of contact and pseudocontact interactions.
45. Gupta RK, Redfield A: **Double nuclear magnetic resonance observation of electron exchange between ferri- and ferrocyclochrome c.** *Science* 1970, **169**:1204–1206, <https://doi.org/10.1126/science.169.3951.1204>.
- Another important early paper setting out the reasons that NMR chemical shifts of substituents of low-spin Fe<sup>3+</sup>-heme are so different from those of diamagnetic hemes.
46. Keller RM, Wüthrich K: **Evolutionary change of the heme c electronic structure: ferricytochrome c-551 from Pseudomonas aeruginosa and horse heart ferricytochrome c.** *Biochem Biophys Res Commun* 1978, **83**:1132–1139, [https://doi.org/10.1016/0006-291X\(78\)91513-9](https://doi.org/10.1016/0006-291X(78)91513-9).
47. Banci L, Bertini I, Luchinat C, Pierattelli R, V Shokhirev N, Walker FA: **Analysis of the temperature dependence of the 1H and 13C isotropic shifts of horse heart ferricytochrome c: explanation of Curie and anti-Curie temperature dependence and nonlinear pseudocontact shifts in a common two-level framework.** *J Appl Collab Syst (JACS)* 1998, **120**:8472–8479, <https://doi.org/10.1021/ja980261x>.
48. Walker FA: **Pulsed EPR and NMR spectroscopy of paramagnetic iron porphyrinates and related iron macrocycles: how to understand patterns of spin delocalization and recognize macrocycle radicals.** *Inorg Chem* 2003, **42**: 4526–4544, <https://doi.org/10.1021/ic026245p>.
- A review covering the use of pulsed EPR, NMR, and DFT calculations to quantify partial spin delocalisation from the Fe<sup>3+</sup>-d-orbitals into orbitals of the porphyrin, including a description of which orbitals are involved in the delocalisation.
49. Liu Q, Zhou X, Liu H, Zhang X, Zhou Z: **Fractional transfer of a free unpaired electron to overcome energy barriers in the formation of Fe<sup>4+</sup> from Fe<sup>3+</sup> during the core contraction of macrocycles: implication for heme distortion.** *Org Biomol Chem* 2015, **13**:2939–2946, <https://doi.org/10.1039/c4ob02429j>.
50. Bren KL: **Going with the electron flow: heme electronic structure and electron transfer in cytochrome c.** *Isr J Chem* 2016, **56**:693–704, <https://doi.org/10.1002/ijch.201600021>.
51. Schweitzer-Stenner R: **Heme–protein interactions and functional relevant heme deformations: the cytochrome c case.** *Molecules* 2022, **27**:8751, <https://doi.org/10.3390/molecules27248751>.
- Extends the Gouterman four-molecular orbital scheme for porphyrins by providing a theoretical treatment of how the Fe<sup>3+</sup>-d-orbitals mix with orbitals of the porphyrin and applies this treatment to understanding EPR and NMR data of low-spin monoheme proteins.
52. Hocking RK, Wasinger EC, Yan YL, Degroot FMF, Walker FA, Hodgson KO, Hedman B, Solomon EI: **Fe L-edge X-ray absorption spectroscopy of low-spin heme relative to non-heme Fe complexes: delocalization of Fe d-electrons into the porphyrin ligand.** *J Appl Collab Syst (JACS)* 2007, **129**: 113–125, <https://doi.org/10.1021/ja065627h>.
- Describes the application of Fe L-edge X-ray absorption spectroscopy to study the delocalization of the Fe d-electrons into the porphyrin (P) ring in terms of both P→Fe σ and π-donation and Fe→P π back-bonding.
53. Ponomarenko N, Niklas J, Pokkuluri PR, Poluektov O, Tiede DM: **Electron paramagnetic resonance characterization of the triheme cytochrome from Geobacter sulfurreducens.** *Biochemistry* 2018, **57**:1722–1732, <https://doi.org/10.1021/acs.biochem.7b00917>.
54. Xavier A, Moura J, Legall J, Dervartanian D: **Oxidation-reduction potentials of the hemes in cytochrome c<sub>3</sub> from Desulfovibrio gigas in the presence and absence of ferredoxin by EPR spectroscopy.** *Biochimie* 1979, **61**:689–695, [https://doi.org/10.1016/s0300-9084\(79\)80167-4](https://doi.org/10.1016/s0300-9084(79)80167-4).
55. Breuer M, Zarzycki P, Shi L, Clarke TA, Edwards MJ, Butt JN, Richardson DJ, Fredrickson JK, Zachara JM, Blumberger J, Rosso KM: **Molecular structure and free energy landscape for electron transport in the decahaem cytochrome MtrF.** *Biochem Soc Trans* 2012, **40**:1198–1203, <https://doi.org/10.1042/BST20120139>.
56. Page CC, Moser CC, Dutton PL: **Mechanism for electron transfer within and between proteins.** *Curr Opin Chem Biol* 2003, **7**:551–556, <https://doi.org/10.1016/j.cbpa.2003.08.005>.
- Thoughtful discussion of the evolutionary pressures on electron transfer proteins within the context of a theoretical description of tunnelling.



57. Edwards PP, Gray HB, Lodge MTJ, Williams RJP: **Electron transfer and electronic conduction through an intervening medium.** *Angew Chem, Int Ed Engl* 2008, **47**:6758–6765, <https://doi.org/10.1002/anie.200703177>.
- A stimulating essay on electron transfer in various materials, including proteins, and the consideration of a protein as a 'large band gap material' with the transferring electron located on a donor dopant and the receiving hole on an acceptor dopant.
58. Winkler JR, Gray HB: **Electron flow through metalloproteins.** *Chem Rev* 2014, **114**:3369–3380, <https://doi.org/10.1021/cr4004715>.
- An authoritative account of electron transfer in proteins through the eyes of leading inorganic chemistry experimentalists.
59. van Wonderen JH, Adamczyk K, Wu X, Jiang X, H Piper SE, Hall CR, Edwards MJ, Clarke TA, Zhang H, C Jeuken LJ, V Sazanovich I, Towrie M, Blumberger J, Meech SR, Butt JN: **Nanosecond heme-to-heme electron transfer rates in a multiheme cytochrome nanowire reported by a spectrally unique His/Met-ligated heme.** *PNAS USA* 2021, **118**, e2107939118, <https://doi.org/10.1073/pnas.2107939118/-/DCSupplemental>.
- Describes the use of protein engineering to break the spectral identity of the hemes of *Shewanella oneidensis* MtrC, followed by covalent attachment of a Ru(II)(bipyridine)<sub>3</sub>-dye to the protein, and the use of pump-probe spectroscopy to determine experimentally for the first time inter-heme electron transfer rates in a MHC.
60. Futera Z, Wu X, Blumberger J: **Tunneling-to-Hopping transition in multiheme cytochrome bioelectronic junctions.** *J Phys Chem Lett* 2023, **14**:445–452, <https://doi.org/10.1021/acs.jpcllett.2c03361>.
61. Futera Z, Ide I, Kayser B, Garg K, Jiang X, Van Wonderen JH, Butt JN, Ishii H, Pecht I, Sheves M, Cahen D, Blumberger J: **Coherent electron transport across a 3 nm bioelectronic junction made of multi-heme proteins.** *J Phys Chem Lett* 2020, **11**:9766–9774, <https://doi.org/10.1021/acs.jpcllett.0c02686>.
- Impressive experimental and computational studies of a Gold-MHC-Gold junction that we suggest provides an example of electronic conductivity via our proposed heme bands.
62. Jiang X, Burger B, Gajdos F, Bortolotti C, Futera Z, Breuer M, Blumberger J: **Kinetics of trifurcated electron flow in the decaheme bacterial proteins MtrC and MtrF.** *Proc Natl Acad Sci U S A* 2019, **116**:3425–3430, <https://doi.org/10.1073/pnas.1818003116>.
63. Zhang Y, Liu C, Balaeff A, Skourtis SS, Beratan DN: **Biological charge transfer via flickering resonance.** *Proc Natl Acad Sci U S A* 2014, **111**:10049–10054, <https://doi.org/10.1073/pnas.1316519111>.
64. Blumberger J: **Recent advances in the theory and molecular simulation of biological electron transfer reactions.** *Chem Rev* 2015, **115**:11191–11238, <https://doi.org/10.1021/acs.chemrev.5b00298>.
- An excellent account of the theory and molecular simulations of biological electron transfer reactions from a leading theoretician in the field.
65. Kanazawa K, Diaz AF, Geiss R, Gill W, Kwak J, Logan A, Rabolt J, Bryan Street G: **“Organic metals”: polypyrrole, a stable synthetic “metallic” polymer.** *Chem Comm* 1979: 854–855, <https://doi.org/10.1039/C39790000854>.
66. Le TH, Kim Y, Yoon H: **Electrical and electrochemical properties of conducting polymers.** *Polymers* 2017, **9**:1–32, <https://doi.org/10.3390/polym9040150>.
67. MacDiarmid AG: **“Synthetic metals”: a novel role for organic polymers (Nobel lecture).** *Angew Chem, Int Ed Engl* 2001, **40**: 2581–2590, [https://doi.org/10.1002/1521-3773\(20010716\)40:14<2581::AID-ANIE2581>3.0.CO;2-2](https://doi.org/10.1002/1521-3773(20010716)40:14<2581::AID-ANIE2581>3.0.CO;2-2).
68. Krishnaswamy S, Ragupathi V, Raman S, Panigrahi P, Nagarajan GS: **Optical properties of P-type polypyrrole thin film synthesized by pulse laser deposition technique: hole transport layer in electroluminescence devices.** *Optik* 2019, **194**, 163034, <https://doi.org/10.1016/j.ijleo.2019.163034>.